Journal of Solid Mechanics Vol. 8, No. 1 (2016) pp. 45-57

Dynamic Stability of Laminated Composite Plates with an External Smart Damper

M. Hoseinzadeh , J. Rezaeepazhand *

Department of Mechanical Engineering , Ferdowsi University of Mashhad , Mashhad, Iran

Received 3 September 2015; accepted 8 December 2015

ABSTRACT

The dynamic stability of a composite plate with external electrorheological (ER) damper subjected to an axial periodic load is investigated. Electrorheological fluids are a class of smart materials, which exhibit reversible changes in mechanical properties when subjected to an electric field. As a result, the dynamic behavior of the structure is changed. The ER damper is used for suppressing the vibrations and improving the stability of the system. The Bingham plastic model is employed to express the behavior of the ER fluid. The finite element model of the structure is developed and constant acceleration average method is used to obtain the response of the system. Effect of different parameters such as the electric field, the orientation of the ER damper, the initial gap between the two electrodes of the ER damper and the stacking sequences of the plate on the first instability boundaries of the composite plate are investigated.

Keywords : Laminated composite; Dynamic buckling; FEA; Smart structures.

1 INTRODUCTION

WHEN a structure is subjected to a periodic compressive load, combinations of the critical values of the load amplitude and excitation frequency may occur, which destabilize the structure. The induced violent vibration is called the dynamic stability or parametric resonance. According to the intrinsic characteristic of the periodic loads, these types of loads may unsatisfactorily affect the dynamic behavior of the structure. Due to the exceptional properties of the composite materials and their importance in stability of the structures, the use of these materials has increased considerably. Consequently, researchers have been increasingly interested in dynamic stability analyses of a composite structure subjected to periodic compressive loads.

Simitses [1] presented a review of the dynamic stability of structures and summarized the three criteria for dynamic buckling load estimation. Moorthy and Reddy[2] investigated the stability of laminated composite plates with transverse shear deformation. The nonlinear dynamic buckling of a rectangular thin elastic plate under a uniaxial harmonic load was investigated by Shivamoggi [3]. The Galerkin finite element model was employed by Chen and Yang [4] for dynamic stability of laminated composite plates subjected to periodic in-plane loads. Kwon[5] presented the comparison of the high-order shear deformation theory and classical theory for dynamic stability analyses of the plate. Sahu and Data [6] investigated the dynamic instability of isotropic, cross-ply and angle-ply laminated composite plates under combined uni-axial and harmonically varying in-plane point or patch loads using the finite element method. The effect of composite patches on dynamic buckling of the perforated cylindrical panels subjected to axial impact load has been studied by Hoseinzadeh and Rezaeepazhand [7]. The results showed that the composite patch can significantly increase the stability of the structure.

*Corresponding author. Tel.: +98 9153114093; Fax: +98 511 8455247.
E-mail address: jrezaeep@um.ac.ir (J. Rezaeepazhand).

Many recent studies have focused on the active vibration control of structures using the electrorheological (ER) fluids. ER fluids are a class of smart materials whose rheological properties are rapidly varied by applying an electric field. When an electric field is applied to an ER fluid, its apparent viscosity reversibly changes in milliseconds.

Numerous experimental studies have been done to investigate mechanical characteristics of ER fluids. Park et al. [8] nvestigated material characteristics of an ER fluid subjected to an electric stimulation and temperature. Lee and Choi[9] presented the dynamic properties of an ER fluid in shear and flow modes. El Wahed et al.[10] described a new approach for analyzing the behavior of ER fluids in squeeze-flow mode, in which the yield stress is determined by minimizing the difference between observed and predicted values of the transmitted force. Nakamura et al. [11] roposed a continuous and accurate viscous control method, for effective use of the ER fluid. They demonstrated the application of the control method to the developed homogeneous ER clutch. The construction, fabrication and performance characteristics of an Electrorheological damper for vibration control of a rotary system have been studied by Patil et al. [12] Sung et al. [13] designed and manufactured a cylindrical type of ER damper based on the required damping force level for a middle-sized passenger vehicle, and experimentally evaluated its field-dependent damping force and dynamic characteristics. The vibration control performance of flow and squeeze mode ER mounts was experimentally compared by Hong et al.[14].

Three rheological regions, pre-yield, yield and post-yield regions, are considered for the quantitative study of ER material behavior. The Kelvin and the Bingham models which express the linear and nonlinear behavior of the ER fluids are usually used in the investigations. The Kelvin model expresses the pre-yield region, while the Bingham model is employed for the post yield behaviour. Due to the considerably low yield stress of these materials, the yield and post yield regions are very important in designing ER devices (Kim et al.[15]). The vibration and dynamic stability of a rectangular plate with an ER fluid core were investigated by Yeh and Chen [16],[17] based on the Kelvin model. The vibration and damping treatment of the sandwich cylindrical panel, including ER fluids as damping materials have been investigated by Mohammadi and Sedaghati [18].

A few researchers have studeid the problem of vibration and dynamic stability of smart structures based on post-yield region behavior of the ER material. Pahlavan and Rezaeepazhand used an electrorheological damper to control transverse vibrations of the cantilever beam [19]. They also used ER fluid as a core of sandwich beams and studied influence of this layer on transient response of the beam [20]. The stability analysis of a smart sandwich beam with cross-ply faces and ER core was investigated by Tabasian and Rezaeepazhand [21]. They used Bingham's model for describing the post-yield behavior of ER fluids. Although there are a few studies that have been devoted to vibration and dynamic stability analysis of smart structures, to the best of authors' knowledge no attempts have been made to investigate the dynamic stability of a laminated plate with external ER damper, especially based on post-yield region behavior of ER material.

In the present study, finite element method is employed to investigate the stability of a laminated plate. In order to improve the dynamic stability of the plate, an external ER damper is applied. In this study, Bingham's model is applied to describe the dynamic behavior of ER fluid. Constant average acceleration method is employed to obtain the transient response of the plate. It is assumed that there is no defect and imperfection in the composite plate.

2 PROBLEM FORMULATION AND SOLUTION METHOD

2.1 Model of the ER fluid

As mentioned before, electric field changes the ER fluid from a Newtonian fluid to a fluid in which polarized particles are aligned in chains. Therefore, the fluid resists against shear forces more firmly. Based on Bingham's model, the shear stress in ER damper is defined in terms of shear rate ($\dot{\gamma}$) and electric field (E) [21]:

$$\tau(E) = \eta\dot{\gamma} + \alpha E^{\beta} \tag{1}$$

α and β are inherent properties of ER fluid, which are usually determined by experiment and η is the viscosity. The particle-type ER fluid used in this study consists of chemical starch particles in silicon oil with constants of the ER fluid $\alpha = 427$ and $\beta = 1.2$ [21]. In addition, the viscosity of this fluid, in the absence of electric field, is obtained equal to 30 *cSt* at room temperature.

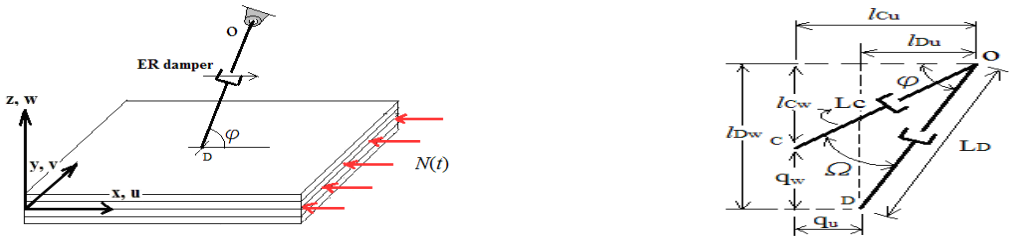

Fig.1
A composite plate with external ER damper subjected to in-plane load .

2.2 Mathematical model of external ER damper

Generally, based on their operation mechanisms and their characteristics, ER dampers have been divided into three different types, shear mode, flow mode and squeeze mode. In the present study, the squeeze mode is used for modelling the ER damper. According to the operation of this mode, the lower electrode is fixed to the base plate, while the upper electrode is free to move up and down along the damper direction. Fig. 1 illustrates the schematic of the plate and external ER damper, used in this study. Since the plate has simply supported boundary conditions in all sides, only the inclination angle φ of the external ER damper is regarded in *x*-*z* plane. In Fig.1, L_D is the length of ER damper before deformation of the plate and l_{Du} and l_{Dw} are the projections of L_D in *x* and *z* directions, respectively. L_C (line oc) and Ω are the time dependent length and inclination angle of the ER damper, respectively. Displacements of the centre point of the plate in *x* and *z* directions are also presented by q_u and q_w which can be obtained by direct integration of the equation of motion. According to Fig. 1, it can be written:

$$\begin{aligned} l_{Cu} &= l_{Du} + q_u \\ l_{Cw} &= l_{Dw} - q_w \end{aligned} \tag{2}$$

where, l_{Cu} and l_{Cw} are the projection of damper length L_C in *x* and *z* axes, respectively. After each time step, the new length of ER damper, L_C, time-dependent inclination angle of the ER damper, Ω, and relative displacement between two electrodes (electrode gap), δ_{Damper}, can be obtained as follows:

$$L_C(t) = \sqrt{l_{Cu}^2 + l_{Cw}^2} \tag{3}$$

$$\Omega(t) = \tan^{-1}\frac{l_{Cw}}{l_{Cu}} \tag{4}$$

$$\delta_{Damper}(t) = L_D - L_C \tag{5}$$

The following relation is used to estimate the characteristics of a squeeze-mode ER damper[19]:

$$F_d(t) = F_v(t) + F_{ER}(t) \tag{6}$$

In which,

$$F_v(t) = \frac{3}{2}\frac{\pi\eta R_{el}^4}{[h_0 + \delta_{Damper}(t)]^3}\dot{\delta}_{Damper}(t)$$

$$F_{ER}(t) = \frac{4}{3}\frac{\pi R_{el}^3}{h_0 + \delta_{Damper}(t)}\tau_y(E)\,\mathrm{sgn}\left(\dot{\delta}_{Damper}(t)\right)$$

In these relations, $F_d(t)$ is the total damping force, $F_v(t)$ is the viscose damping force and $F_{ER}(t)$ is the controllable damping force associated with applied electric field. R_{el} is the radius of each circular electrode, and η is the basic viscosity of the fluid, when the electric field is zero. h_0 denotes the initial gap between the electrodes. $\dot{\delta}_{Damper}(t)$ is the relative velocity of the two electrodes. According to the proposed ER damper, the applied electric field is as follows[22]:

$$E(t)=\frac{V(t)}{\delta_{Damper}(t)} \tag{7}$$

where $V(t)$ is the applied voltage.

2.3 FE modelling of the structure

The relations between deformations and applied forces and moments of a composite laminated plate is expressed as follows:

$$\begin{Bmatrix}\{N\}\\ \{M\}\end{Bmatrix}=\begin{bmatrix}[A] & [B]\\ [B] & [D]\end{bmatrix}\begin{Bmatrix}\{\varepsilon^0\}\\ \{\kappa\}\end{Bmatrix} \tag{8}$$

In which, $\{\{N\}\}=\{N_x \quad N_y \quad N_{xy}\}^T$, $\{\{M\}\}=\{M_x \quad M_y \quad M_{xy}\}^T$, $\{\{\varepsilon^0\}\}=\{\varepsilon_x^0 \quad \varepsilon_y^0 \quad \varepsilon_{xy}^0\}^T$ and $\{\{\kappa\}\}=\{\kappa_x \quad \kappa_y \quad \kappa_{xy}\}^T$. Moreover, $[A]$, $[B]$ and $[D]$ are 3×3 stiffness matrices of the laminate which are defined as follows:

$$\begin{aligned}A_{ij}&=\sum_{k=1}^{n}(\bar{Q}_{ij})_k\,(z_k-z_{k-1})\\ B_{ij}&=\frac{1}{2}\sum_{k=1}^{n}(\bar{Q}_{ij})_k\,(z_k{}^2-z_{k-1}{}^2)\\ D_{ij}&=\frac{1}{3}\sum_{k=1}^{n}(\bar{Q}_{ij})_k\,(z_k{}^3-z_{k-1}{}^3)\end{aligned} \tag{9}$$

where, z_k is the height of the top plane of k layer from the mid-plane of the laminated face, and $\bar{Q}_{ij}$ are components of the transformed reduced stiffness matrix of each lamina.

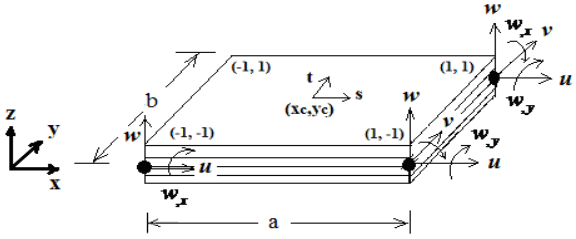

Fig.2
Four nodes rectangular element and its degrees of freedom.

As illustrated in Fig. 2, a four nodes rectangular element is considered for the finite element analyses. u, v and w are the displacements in x, y and z directions and $w_{,x}$ and $w_{,y}$ are the rotations about y and x directions, respectively. The strain–displacement relations of the laminated plate can be expressed as:

$$\{\varepsilon\}=\{\varepsilon^0\}-z_i\,\{\kappa\},\ i=1,...,n \tag{10}$$

where, $\{\varepsilon^0\}=\{u_{,x}, v_{,y}, u_{,y}+v_{,x}\}^T$, $\{\kappa\}=\{w_{,xx}, w_{,yy}, 2w_{,xy}\}$ and n is the number of lamina. Displacement vector of the element is written as:

$$\begin{Bmatrix} u \\ v \\ w \end{Bmatrix} = [N]\{q\} = \begin{bmatrix} N_u \\ N_v \\ N_w \end{bmatrix}\{q\}$$
$$\{q\} = \{u_i, v_i, w_i, w_{,yi}, w_{,xi}\}^T, \quad i=1,...,4 \tag{11}$$

In which, $[N]$ is a 3×20 matrix and q is the element degrees of freedom vector. N_u, N_v and N_w are the shape function matrices corresponding to the deformation u, v and w.

In order to find the equation of motion of the composite laminated plate subjected to periodic in-plane load, Hamilton's principle is employed. Therefore, the strain energy (V), kinetic energy (T) and the work (W) done by in-plane load must be obtained.

The strain energy of the composite laminated plate can be written as:

$$V = \frac{1}{2}\int_v \{\varepsilon\}^T\{\sigma\}dv = \frac{1}{2}\int_A \begin{Bmatrix} \{\varepsilon^0\} \\ \{\kappa\} \end{Bmatrix}^T \begin{bmatrix} [A] & [B] \\ [B] & [D] \end{bmatrix} \begin{Bmatrix} \{\varepsilon^0\} \\ \{\kappa\} \end{Bmatrix} dA \tag{12}$$

where,

$$\{\varepsilon^0\} = [R]\{q\},\ \{\kappa\} = [S]\{q\}$$
$$[R] = \begin{bmatrix} 1/a\,(\partial/\partial s) & 0 & 0 \\ 0 & 1/b\,(\partial/\partial t) & 0 \\ 1/b\,(\partial/\partial t) & 1/a\,(\partial/\partial s) & 0 \end{bmatrix}[N]$$
$$[S] = \begin{bmatrix} 0 & 0 & -1/a^2\,(\partial^2/\partial s^2) \\ 0 & 0 & -1/b^2\,(\partial^2/\partial t^2) \\ 0 & 0 & -2/(ab)\,(\partial^2/\partial s\,\partial t) \end{bmatrix}[N] \tag{13}$$

Eq. (12) can be rewritten as:

$$V = \frac{1}{2}\{q\}^T[K^{(e)}]\{q\}$$
$$[K^{(e)}] = \int_A \left([R]^T[A][R] + [R]^T[B][S] + [S]^T[B][R] + [S]^T[D][S]\right)dA \tag{14}$$

where, $[K^{(e)}]$ is the element stiffness matrix of the laminated composite plate.

Neglecting the shear deformation and rotary inertia of the laminate, the kinetic energy of laminated plate due to in-plane and transverse displacements is obtained:

$$T = \frac{1}{2}\int_A \left[\rho h\,(\dot{u}^2 + \dot{v}^2 + \dot{w}^2)\right]dA \tag{15}$$

In which, ρ is the density and h is the thickness of the plate. Substitution of Eq. (11) into Eq. (15), gives:

$$T = \frac{1}{2}\{\dot{q}\}^T \left[M^{(e)}\right]\{\dot{q}\}$$
$$\left[M^{(e)}\right] = \int_A \rho h \left(\left[N_u\right]^T \left[N_u\right] + \left[N_v\right]^T \left[N_v\right] + \left[N_w\right]^T \left[N_w\right]\right) dA \tag{16}$$

where, $\left[M^{(e)}\right]$ is the element mass matrix. The work done by the in-plane load $N(t)$, can be written as [17],[21]:

$$W = \frac{1}{2}\{q\}^T N(t)\left[K_g^{(e)}\right]\{q\}$$
$$\left[K_g^{(e)}\right] = \int_A \left[\frac{dN_w}{dx}\right]^T \left[\frac{dN_w}{dx}\right] dA \tag{17}$$

where, $\left[K_g^{(e)}\right]$ is the element geometric stiffness matrix.

Substitution of T, V and W into Hamilton's principle gives the equation of motion of the composite plate subjected to time depending in-plane load, as follows:

$$\left[M^{(e)}\right]\{\ddot{q}\} + \left(\left[K^{(e)}\right] - N(t)\left[K_g^{(e)}\right]\right)\{q\} = \{0\} \tag{18}$$

The in-plane load is periodic and can be expressed in the form:

$$N(t) = N_t \cos \omega t \tag{19}$$

where N_t is the amplitude of the dynamic portion of $N(t)$ and ω is the excitation frequency.

Neglecting structural damping effects, the plate does not have any damping property by itself and the only damping force is exerted by the external ER damper to the point of the plate where the smart damper is attached (Fig. 1). As mentioned before, there are two components in the ER damper that can affect the damping of the structure. The first component, $F_v(t)$, is proportional to relative velocity of the electrodes, which is considered the same as velocity of the center point of the plate. Hence, this component of damping emerges in $[C]$ matrix in general form of equation of motion. The second component of ER damper, $F_{ER}(t)$, which is proportional to the sign of velocity enters to the model as an equivalent time-dependent Coulomb damping $[D]$. Considering the influence of these two damping components the following general form of equation of motion of plate with external smart damper is achieved:

$$[M]\{\ddot{q}\} + [C]\{\dot{q}\} + \left([K] - N_t \cos \omega t\ [K_g]\right)\{q\} = -[D]\ \mathrm{sgn}\{\dot{q}\} \tag{20}$$

It is apparent that the terms $C_u^{ER}, C_w^{ER}, D_u^{ER}$ and D_w^{ER} are corresponding to the damping components of the point in the plate which damper is attached (see Fig. 1). Hence, all other components of $[C]$ and $[D]$ matrices are equal to zero. Ω is the time dependent inclination angle of the ER damper.

2.4 Solution method

In order to obtain the response of the smart structure subjected to periodic load, constant average acceleration method, which is a stable case of the Newmark family, is employed. In this method, the total solution time is divided into several intervals, and the solution is done step by step [23]. In each step, the values of displacement, velocity and acceleration are calculated in terms of their values in the pervious steps. Applying this method to Eq. (20), a recursive formula is obtained, which calculates the vector $\{q\}$ based on its values in the previous steps. Considering the general form of equation of motion as $[M]\{\ddot{q}\}_{t+\Delta t} + [C]\{\dot{q}\}_{t+\Delta t} + [K]\{q\}_{t+\Delta t} = \{F\}_{t+\Delta t}$, the procedure can be summarized as follows:

1. Calculate $[K]$, $[M]$ and $[C]$ matrices.

2. $\{\ddot{q}\}_0$ is calculated using $\{q\}_0$ and $\{\dot{q}\}_0$: $[M]\{\ddot{q}\}_0 = \{F\} - [K]\{q\}_0 - [C]\{\dot{q}\}_0$
3. Choosing Δt, $\delta = 0.5$ and $\alpha = 0.25 \times (0.5+\delta)^2$, the following constants are computed:

$$c_0 = \frac{1}{\alpha \Delta t^2}, c_1 = \frac{\delta}{\alpha \Delta t}, c_2 = \frac{1}{\alpha \Delta t}, c_3 = \frac{1}{2\alpha} - 1, c_4 = \frac{\delta}{\alpha} - 1, c_5 = \frac{\Delta t}{2}\left(\frac{\delta}{\alpha} - 2\right), c_6 = \Delta t\,(1-\delta), c_7 = \delta \Delta t$$

4. Form the effective stiffness matrix $[\hat{K}] = [K] + c_0[M] + c_1[C]$
5. For each time step:

Calculate the effective load at time $t + \Delta t$:

$$\{\hat{F}\}_{t+\Delta t} = \{F\}_{t+\Delta t} + [M]\left(c_0\{q\}_t + c_2\{\dot{q}\}_t + c_3\{\ddot{q}\}_t\right) + [C]\left(c_1\{q\}_t + c_4\{\dot{q}\}_t + c_5\{\ddot{q}\}_t\right)$$

Solve for $\{q\}_{t+\Delta t}$: $[\hat{K}]\{q\}_{t+\Delta t} = \{\hat{F}\}_{t+\Delta t}$

Calculate the accelerations and velocities at time $t + \Delta t$:

$$\{\ddot{q}\}_{t+\Delta t} = c_0\left(\{q\}_{t+\Delta t} - \{q\}_t\right) - c_2\{\dot{q}\}_t - c_3\{\ddot{q}\}_t$$
$$\{\dot{q}\}_{t+\Delta t} = \{\dot{q}\}_t + c_6\{\ddot{q}\}_t + c_7\{\ddot{q}\}_{t+\Delta t}$$

By employing the constant average acceleration method, the transient response of the plate for different load is obtained. The dynamic stability load of the structure can be achieved by plotting the values of maximum deflections of the plate versus the load amplitudes. In another word, the critical state and the dynamic buckling load would be estimated from the junction of asymptotic of the displacement curve and the load axis.[21]

The derived finite element model and the solution procedure are programmed as a code. In the next section, after validation of the model, the effects of different parameters on the stability region of the laminated composite plate are presented.

3 RESULTS AND DISCUSSION

To improve the stability regions of the cross-ply composite plate, a simply supported square plate with external ER damper, as shown in Fig. 1, is considered. The structural geometric properties of the composite plate, used in the present analyses, are as follows:

$$a = b = 0.5m, h = a/100, E_1 = 132.5\ \text{GPa}, E_2 = 10.8\ \text{GPa}, G_{12} = G_{13} = 5.7\ \text{GPa}, G_{23} = 3.4\ \text{GPa}, \nu_{12} = \nu_{13} = 0.24, \rho = 1540\ \text{Kg}/m^3$$

The radius and the initial gap of the electrodes of the circular ER damper are R_{el}=0.02 *m* and h_0=0.01 *m*, respectively (unless otherwise mentioned). The non-dimensional excitation frequency $\bar{\Omega} = \omega a^2 \sqrt{\rho h / D_0}$ is used throughout the dynamic stability analysis, in which $D_0 = E_1 h^3 / 12\left(1 - \nu_{12}\nu_{21}\right)$. Before investigating the effect of different parameters, it is necessary to compare the results with available published works to validate the finite element code and the method of finding buckling load.

3.1 Validation of the model

Due to the lack of the published works for dynamic stability of a laminated plate with external ER damper, the mathematical model of the ER damper and the present FE code for dynamic stability of the laminated plate are validated separately.

For validation of the ER damper model, the transmitted forces of the ER damper are compared with the experimental results of Jung et al. [22] in Table 1. The experiment was implemented on a squeeze-mode ER damper,

including a coil spring subjected to a harmonic excitation force. Small discrepancy between the numerical and experimental results can be explained by neglecting the coil spring mass in the present study.

Table 1
Comparison of the transmitted force (*N*) obtained in this study with experiments [22]

Voltage (kV)	1	2	3	4
This study	0.54	1.24	2.01	2.8
Ref.[22]	0.60	1.25	2.05	2.7

In order to evaluate the dynamic stability of the cross-ply laminated plate, the first instability boundary achieved by the present method is compared with the results of Moorthy and Reddy [2] in Fig.3. They employed the Bolotin's method for obtaining the first stability region of the composite plate subjected to harmonic load $N(t) = N_t \cos \omega t$. In their work, only the two first terms of the Fourier series are considered. In Fig.3, dynamic load factor (DLF) is the ratio of dynamic buckling load to the static buckling load. According to this Figure, the present result of the stability region is very close to the 2nd approximation of the Moorthy and Reddy[2]. It should be noted that the minimum point of the first instability region occurs at the frequency equals two times of the first natural frequency of the system.

As observed in Fig. 3, appropriate convergence achieved between results and it can be concluded that the presented method of finding critical load and corresponding instability boundary is accurate.

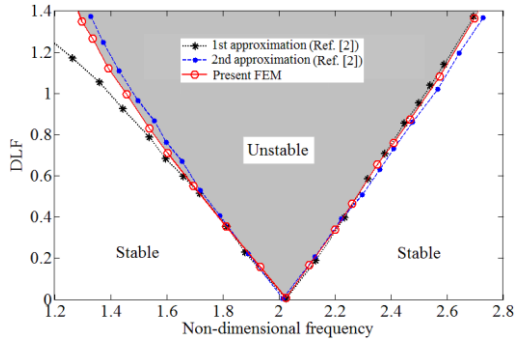

Fig.3
The first instability region of the laminated plate $(0/90)_s$.

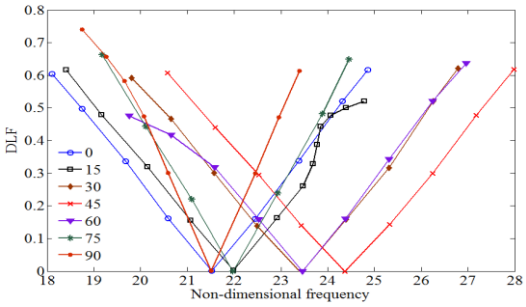

Fig.4
Effect of ply orientations on the first instability region of the orthotropic plate (ϑ).

3.2 Effect of fiber orientation in orthotropic plate

To investigate the effect of fiber orientation on the instability regions of the plate, an orthotropic plate is considered. Fig. 4 shows the effect of different fiber orientation on the first instability region of the orthotropic plates. As depicted, by increasing the fiber orientation up to 45°, the minimum point of the instability region moves to the higher frequencies. However, for higher fiber angles $45^\circ < \theta < 90^\circ$ the instability regions move back to smaller frequencies. The instability regions of fiber angles θ and $90-\theta$ (*i.e.* 0 and 90, 15 and 75, 30 and 60) start from a similar frequency. However, this region is smaller for fiber angles 75° and 90°. Another observation is that for an orthotropic plate, the maximum shift of frequency occurs for the fiber angle of 45° with maximum area of the instability region.

In the next sections, effects of different parameters on the first instability region of the cross-ply laminated plate with external ER damper are discussed.

3.3 Influence of applying constant voltages into electrodes

The first instability region of the system for some constant levels of the applied voltage is examined for symmetric and anti-symmetric cross ply laminated plates. The inclination angle φ is assumed to be 90^{o} and the characteristics of the ER damper are as indicated in previous sections. The results are depicted in Figs. 5 and 6, respectively. As illustrated in these Figures, increase in the applied voltage enhances the stability of the structure. This enhancement is more noticeable for symmetric laminated. In another word, in similar conditions for the symmetric and anti-symmetric laminated plates an external ER damper has more influence on the stability of the symmetric laminates. As illustrated in Figs. 5 and 6, the normalized frequency of the anti-symmetric structure is less than the symmetric one. Smaller frequency in the anti-symmetric laminated plate is caused by its lower stiffness. Consequently, for anti-symmetric configuration, higher voltage is needed to produce instability boundaries similar to the symmetric one. It should be noted again that all the parameters except the fiber angles are identical for the symmetric and anti-symmetric structures. Another conclusion that can be observed in from Figs. 5 and 6 is that the maximum discrepancy between the various instability boundaries occurs around the frequency of the minimum point of instability region of the plate.

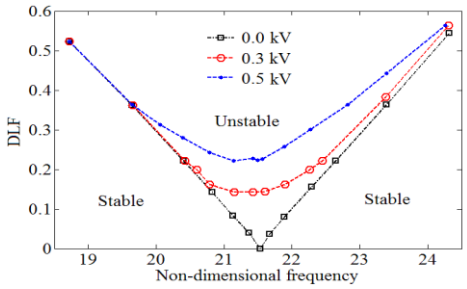

Fig.5
Effect of applied voltages on the first instability region of the symmetric laminated plate $(0/90)_s$.

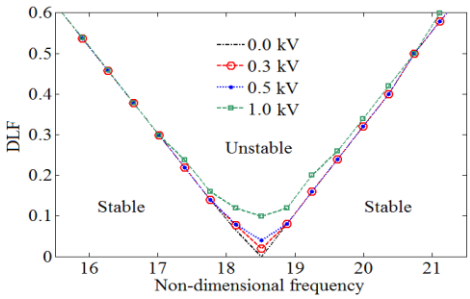

Fig.6
Effect of applied voltages on the first instability region of the anti-symmetric laminated plate $(0_2/90_2)$.

3.4 Influence of the ER damper orientation

In order to investigate the effect of damper inclination angle, different damper angles, 45, 60, 75, 80 and 90, are considered. The first instability regions corresponding to these cases are obtained and illustrated in Fig. 7 for symmetric cross ply laminated plate, when 0.3 kV is applied into the electrodes. As illustrated in Fig. 7, increasing the damper angle gives an upward rise to the instability boundary and consequently, improves the stability of the system. The instability boundaries are similar for high inclination angles $80^{\circ} \le \theta \le 90^{\circ}$. In another word, there is a 10° freedom for mounting the ER damper in the structure. Another conclusion which can be observed from Fig. 7 is that, in smaller frequencies, the instability boundaries are fully coincided, while there is a small discrepancy between instability boundaries in higher frequencies. Fig. 8 presents the effect of the ER damper inclination angle on the first instability region of the anti-symmetric cross ply laminated plate. To compare the result of inclination angle for symmetric and anti-symmetric laminates, similar conditions are considered for both cases. Clearly, the inclination angle does not have significant effect on the instability boundary of the anti-symmetric configuration.

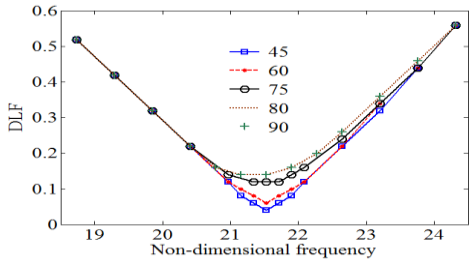

Fig.7
Effect of damper inclination angle on the first instability region of the symmetric laminated plate $(0/90)_s$.

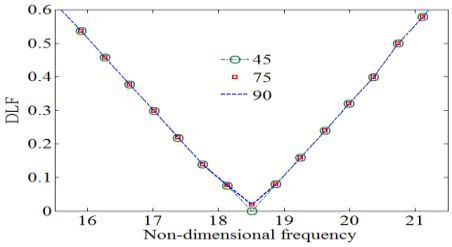

Fig.8
Effect of damper inclination angle on the first instability region of the anti-symmetric laminated plate $(0_2/90_2)$.

4.4 Influence of the initial gap of the electrodes

For squeeze mode ER damper, the initial gap between the two electrodes can significantly affect the stability of the structure. The instability boundaries of the symmetric and anti-symmetric cross ply laminated plates for different initial gaps (0.005, 0.006, 0.007, 0.010 and 0.015 *m*) are presented in Figs. 9 and 10, respectively. A 0.3 kV is applied into the electrodes in these cases. According to these Figures, the smaller initial gap yields to more stability of the system. Furthermore, for a 0.015 *m* initial gap the instability boundary is similar to the instability region of the plate without an ER damper. In another word, the effect of ER damper is reduced for higher initial gaps. Consequently, higher values of voltage are required to produce the same level of stability by increasing the initial gap. As it can be observed, the change in the initial gap has more effect on the instability region of the symmetric laminated plate in comparison to the anti-symmetric one.

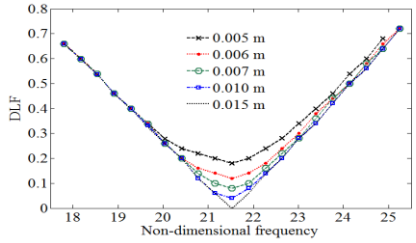

Fig.9
Effect of initial gap on the first instability region of the symmetric laminated plate $(0/90)_s$.

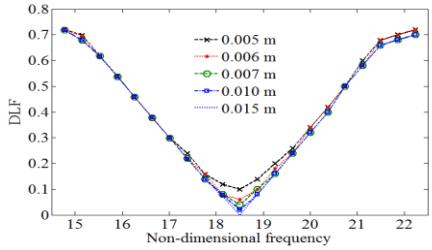

Fig.10
Effect of initial gap on the first instability region of the anti-symmetric laminated plate $(0_2/90_2)$.

4.5 Influence of the electrode radius

Figs. 11 and 12 illustrate the effect of electrode radius on the first instability boundary of the symmetric and anti-symmetric cross ply laminated plates. In these Figures as it was expected, the larger electrode radius yields to an

upward movement of the instability boundary and consequently, increases the stability of the system. Similar to the effect of the initial gap, more enhancements are observed for the symmetric laminated than the anti-symmetric one. Although this trend can be satisfactory, there is a critical value for the geometric characteristics of the ER damper. It is apparent that the designer must consider the geometric limitations and economical aspects. Therefore, the material properties of the structure and the ER damper should be considered in designing the squeeze-mode ER damper.

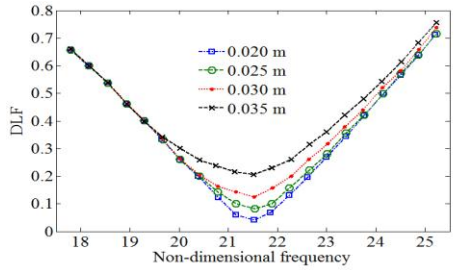

Fig.11
Effect of electrode radius on the first instability region of the symmetric laminated plate $(0/90)_s$.

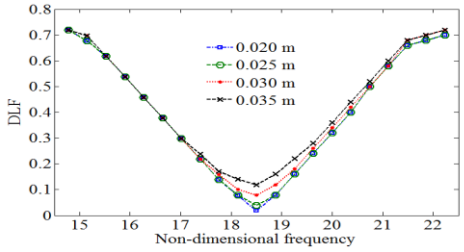

Fig.12
Effect of electrode radius on the first instability region of the anti-symmetric laminated plate $(0_2/90_2)$.

4.6 Influence of stacking sequences of the laminate

As demonstrated in previous sections, the stacking sequence of laminates can affect the instability of boundaries on the composite plate. It has been observed that the smart damper is more effective for symmetric laminates. Hence, the effect of stacking sequence on the dynamic buckling load of the cross-ply symmetric laminated plate with an ER damper is considered in this section. As illustrated before, the DLF of the minimum point of the first instability region is changed for different stacking sequence $(90_{12-n}/0_n)_s$ (n=2,3,...,12) which n denotes the number of 0° layers. Clearly, the DLF of the composite plate increases by an increase in the applied voltage. In a constant voltage, generally, the DLF decreases when the number of the 0° layers increased.

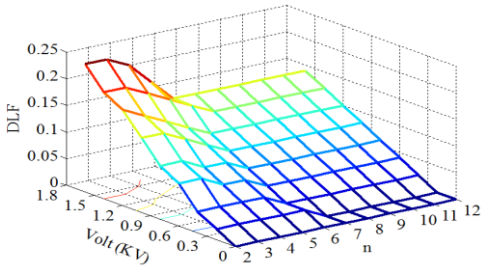

Fig.13
Effect of applied voltage and the number of 0° layers on the minimum point of the first instability region $(90_{12-n}/0_n)_s$.

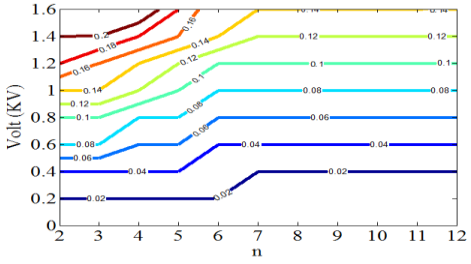

Fig.14
Contours of the dynamic load factor (DLF) for different voltages and the number of 0° layers $(90_{12-n}/0_n)_s$.

5 CONCLUSIONS

The dynamic stability of a simply supported laminated composite plate with an ER damper is considered in this paper. A finite element model for the plate and the ER damper has been derived, and the constant average acceleration algorithm has been used to simulate the time dependent behavior of the structure. Due to the considerably low yield stress of ER fluids and their characteristics in the post-yield region, the Bingham plastic model is used to derive the finite element model of the composite plate with external ER damper. The presented numerical results illustrated that the effects of external ER damper tend to stabilize the plate subjected to dynamic in-plane compressive load. The results indicated that, the applied electric field, the inclination angle of the ER damper, the initial gap between the two electrodes and the radius of the damper have considerable effect on damping treatment and consequently, the stability of the structure. It has been observed that the first instability boundaries of the structure increases by increasing the applied voltage, inclination angle and the radius of the damper electrodes. Furthermore, reduction in the initial gap results in upward movement of the instability region. Moreover, the applied voltage can increase the stability of the system. This increment is higher when the symmetric stacking sequences are used. It is also concluded that, increasing the number of 0° layers, up to a certain number of layers, decreases the dynamic load factor.

REFERENCES

[1] Simitses G.J., 1987, Stability of dynamically loaded structures, *Applied Mechanics Reviews* **40**(10): 1403-1408.

[2] Moorthy J., Reddy J.N., 1990, Parametric instability of laminated composite plates with transverse shear deformation, *International Journal of Solids Structures* **26**(7): 801-811.

[3] Shivamoggi B. K., 1977, Dynamic buckling of thin elastic plate: nonlinear theory, *Journal of Sound and Vibration* **54** (l) : 75-82.

[4] Chen L.W., Yang J.Y., 1990, Dynamic stability of laminated composite plates by the finite element method, *Computers and Structures* **36**(5): 845-851.

[5] Kwon Y.W., 1991, Finite element analysis of dynamic instability of layered composite plates using a high-order bending theory, *Computers and Structures* **38**(1): 57-62.

[6] Sahu S.K., Datta P.K., 2000, Dynamic instability of laminated composite rectangular plates subjected to non-uniform harmonic in-plane edge loading, in: Proceedings of the IMECH E Part G, *Journal of Aerospace Engineering* **214**(5): 295-312.

[7] Hoseinzadeh M., Rezaeepazhand J., 2011, Dynamic buckling of perforated metallic cylindrical panels reinforced with composite patches, *Journal of Reinforced Plastics and Composites* **30**(18): 1519-1528.

[8] Park W.C., Choi S.B., Suh M.S., 1999, Material characteristics of an ER fluid and its influence on damping forces of an ER damper Part II: damping forces, *Materials and Design* **20**: 325-330.

[9] Lee H.G., Choi S.B., 2002, Dynamic properties of an ER fluid under shear and flow modes, *Materials and Design* **23**: 69-76.

[10] El Wahed A.K., Sproston J.L., Stanway R., Williams E.W., 2003, An improved model of ERfluids in squeeze-flow through model updating of the estimated yield stress, *Journal of Sound and Vibration* **268**: 581-599.

[11] Nakamura T., Saga N., Nakazawa M., 2004, Variable viscous control of a homogeneous ER fluid device considering its dynamic characteristics, *Mechatronics* **14**: 55-68.

[12] Patil S.S., Gawade S.S., Patil S.R., 2011, Electrorheological Fluid Damper for Vibration Reduction in Rotary System, *International Journal of Fluids Engineering* **3**(3): 325-333.

[13] Sung K.G., Han Y.M., Cho J.W., Choi S.B., 2008, Vibration control of vehicle ER suspension system using fuzzy moving sliding mode controller, *Journal of Sound and Vibration* **311**: 1004-1019.

[14] Hong S. R., Choi S. B., Lee D. Y., 2006, Comparison of vibration control performance between flow and squeeze mode ER mounts: Experimental work, *Journal of Sound and Vibration* **291** :740-748.

[15] Kim J., Kim J.Y., Choi S.B.,2003, Material characterization of ER fluids at high frequency, *Journal of Sound and Vibration* **267** : 57-65.

[16] Yeh J. Y., Chen L. W., 2004, Vibration of a sandwich plate with a constrained layer and electrorheological fluid core, *Composite Structures* **65**: 251-258.

[17] Yeh J.Y., Chen L.W., 2005, Dynamic stability of a sandwich plate with a constraining layer and electrorheological fluid core, *Journal of Sound and Vibration* **285**: 637-652.

[18] Mohammadi F., Sedaghati R., 2012, Vibration analysis and design optimization of sandwich cylindrical panels fully and partially treated with electrorheological fluid materials, *Journal of Intelligent Material Systems and Structures* **23:** 1679-1697.

[19] Pahlavan L., Rezaeepazhand J., 2007, Dynamic response analysis and vibration control of a cantilever beam with a squeeze-mode electrorheological damper, *Smart Materials and Structures* **16**: 2183-2189.

[20] Rezaeepazhand J., Pahlavan L., 2009, Transient response of sandwich beams with electrorheological core, *Journal of Intelligent Material Systems and Structures* **20**: 171-179.
[21] Tabassian R., Rezaeepazhand J., 2012, Stability of smart sandwich beams with cross-ply faces and electrorheological core subjected to axial load, *Journal of Reinforced Plastics and Composites* **31**: 55-64.
[22] Jung W.J., Jeong W.B., Hong S.R., Choi S.B., 2004, Vibration control of a flexible beam structure using squeeze-mode ER mounts, *Journal of Sound and Vibration* **273**: 185-199.
[23] Owen D.R.J., Hinton E., 1980, *Finite Elements in Plasticity: Theory and Practice,* Pineridge Press, Swansea.